

1 Epigenome-wide association study of pregnancy exposure to green space and 2 placental DNA methylation

3 *Sofía Aguilar-Lacasaña^{a,b,c,d#}, Marta Cosin-Tomas^{a,c,d}, Bruno Raimbault^{a,b,c}, Laura*
4 *Gómez^{a,b,c,d}, Olga Sánchez^{e,f}, Maria Julia Zanini^g, Rosalia Pascal Capdevila^{f,h}, Maria*
5 *Forasterⁱ, Mireia Gascon^{a,c,d,j}, Ioar Rivas^{a,c,d}, Elisa Llurba^{e,g}, Maria Dolores Gómez-*
6 *Roig^{f,h}, Jordi Sunyer^{a,c,d}, Mariona Bustamante^{a,c,d*#}, Martine Vrijheid^{a,c,d*}, Payam*
7 *Dadvand^{a,c,d*}*

8 a ISGlobal, Barcelona, Spain; b Facultat de Biologia, Universitat de Barcelona (UB), Barcelona, Spain; c Universitat Pompeu Fabra (UPF), Barcelona,
9 Spain; d CIBER Epidemiología y Salud Pública, Instituto de Salud Carlos III, Spain; e Primary Care Interventions to Prevent Maternal and Child Chronic
10 Diseases of Perinatal and Developmental Origin Network (RICORS-SAMID) (RD21/0012/0001); f Primary Care Interventions to Prevent Maternal and
11 Child Chronic Diseases of Perinatal and Developmental Origin Network (RICORS-SAMID) (RD21/0012/0003); g Department of Obstetrics and
12 Gynaecology. Institut d'Investigació Biomèdica Sant Pau - IIB Sant Pau. Hospital de la Santa Creu i Sant Pau, Barcelona, Spain; h BCNatal (Hospital
13 Sant Joan de Déu and Hospital Clínic de Barcelona); i Institut de Recerca Sant Joan de Déu (IR-SJD), Barcelona, Spain; j PHAGEX Research Group,
14 Blanquerna School of Health Science, Universitat Ramon Llull (URL), Barcelona, Spain; k Unitat de Suport a la Recerca de la Catalunya Central,
15 Fundació Institut Universitari per a la Recerca a l'Atenció Primària de Salut Jordi Gol i Gurina (IDIAPJGol), Manresa, Spain

16 * Joint last authors

17 #Corresponding authors: sofia.aguilar@isglobal.org; mariona.bustamante@isglobal.org

Abbreviations: ADCY4: Adenylate Cyclase 4 gene; AIP: Aryl Hydrocarbon Receptor Interacting Protein; BiSC: Barcelona Life Study Cohort; BMIQ: Beta-mixture quantile; BN: Bonferroni; Bp: base pairs; C3orf55: Solute Carrier Family 66 Member 1 Like, Pseudogene; CpG: Cytosine-phosphate-guanine; COPD: chronic obstructive pulmonary disease; DMP: Differentially methylated position; DMR: Differentially methylated region; DNAm: DNA methylation; IQR: Interquartile range; eQTM: Expression quantitative methylated regions; ESCAPE: European Study of Cohorts for Air Pollution Effects; Enh: Enhancer; EWAS: Epigenome-wide association study; gDMR: Germline differently methylated region; GLRB: Glycine Receptor Beta gene; GPS: Global Positioning System; GS: Green space; GO: Gene Ontology; HSPA1B: Heat Shock Protein Family A (Hsp70) Member 1B gene; HTR2A: 5-Hydroxytryptamine Receptor 2A gene; HUGO: Human Genome facility; ICGC: Cartographic and Geology Institute of Catalonia; KEGG: Kyoto Encyclopedia of Genes and Genomes; LOX: Lysile Oxidase gene; LUR: Land Use Regression Models; mQTL: methylation Quantitative Trait Loci; mtDNAC: mitochondria DNA content; NR2E1: Nuclear Receptor Subfamily 2 Group E Member 1 2; OSBPL9: Oxysterol Binding Protein Like 9 gene; PCA: Principal Component Analysis; PDE8A: Phosphodiesterase 8A gene; PM2.5: Particulate matter with aerodynamic diameter 2.5 microm; PMD: Partially methylated domain; QC: Quality control; R: Red values; MAF: minor allele frequency; NIR: near infrared values; NDVI: Normalized Difference Vegetation Index; SKA1: Spindle And Kinetochore Associated Complex Subunit 1 gene; SLC25A10: Solute carrier family 25 member 10

NOTE: This preprint reports new research that has not been certified by peer review and should not be used to guide clinical practice.

flanking active transcription start site; UCSC: University of California, Santa Cruz; UTR: untranslated region; ZNF22: Zinc Finger Protein 22; ZNF22-AS1: Zinc Finger Protein 22 Antisense RNA 1; ZNF562: Zinc Finger Protein 562 gene.

18 **Abstract**

19 Maternal exposure to green space during pregnancy has been associated with lower risk
20 for adverse birth outcomes; however, the underlying biological mechanisms remain
21 largely unknown. Epigenetic changes, such as DNA methylation (DNAm), might be one
22 of the molecular mechanisms contributing to this association. The placenta is the key
23 organ for foetal growth and development, but studies of prenatal green space exposure
24 and placental DNAm are scarce and have not been conducted on a genome-wide scale.
25 Here, we aimed to investigate the association between exposure to green space during
26 pregnancy and epigenome-wide placental DNAm.

27 This study was conducted in 550 mother-child pairs from the Barcelona Life Study Cohort
28 (BiSC), a population-based birth cohort in Spain (2018-2021). We comprehensively
29 assessed green space exposure during pregnancy as (i) residential surrounding greenness
30 (satellite-based Normalized Difference Vegetation Index (NDVI) in buffers of 100m,
31 300m and 500m), (ii) residential distance to the nearest major green space (meters), iii)
32 use of green space (hours/week), and iv) visual access to greenery through home window
33 (\geq half of the view). Placental DNAm was measured with the EPIC array. To identify
34 differentially methylated positions (DMPs), we fitted robust linear regression models
35 adjusted for relevant covariates, while differentially methylated regions (DMRs) were
36 identified using the *dmrff* method.

37 After Bonferroni (BN) correction, cg14852540, annotated to *SLC25A10* gene, was
38 inversely associated with residential surrounding greenness within 500m buffer.
39 Additionally, ten unique DMRs were associated with surrounding greenness within 300m
40 and 500m, distance or visual access to green space. No associations were found for
41 surrounding greenness within 100m or use of green space. Genes annotated to these loci
42 are involved in transcriptional regulation, metabolism and mitochondrial respiration.

43 Overall, we identified associations between prenatal green space exposure and DNAm
44 levels in placenta. Further research is needed to validate these results and understand the
45 underlying biological pathways.

46 **Key words:** green space, DNA methylation, placenta, EWAS, DMR, pregnancy

47 **1. Introduction**

48 Exposure to green space has been associated with health benefits over the entire life-
49 course (Hu et al., 2021; Y. Yuan et al., 2020; Zare Sakhvidi et al., 2023). Specifically,
50 prenatal exposure to green space has been associated with lower risk of adverse birth
51 outcomes such as low birthweight (Nieuwenhuijsen et al., 2019; Torres Toda et al., 2022).
52 Mechanistically, potential pathways underlying these associations include capacity
53 instoration (e.g., encouraging physical activity and increasing social cohesion), harm
54 mitigation (e.g., improving air quality, reducing noise, and dissipating heat, reducing
55 exposure to air pollution, noise, and heat), capacity restoration (e.g., reducing stress and
56 renewing attention) and immunity improvement (e.g., by enriching the microbiome)
57 (Bowyer et al., 2022; Cruells et al., 2024; Markevych et al., 2017).

58 Epigenetic changes may be one of the molecular mechanisms contributing to the
59 association between prenatal green space exposure and lower risk of adverse birth
60 outcomes, either directly or indirectly through the aforementioned pathways. The
61 epigenome comprises all modifications to DNA, or to DNA-associated RNA and
62 proteins, that permit interpretation of the genome to instruct cell identity and function
63 (Hemberger et al., 2020). These modifications ultimately influence gene expression.
64 Among all epigenetic marks, DNA methylation (DNAm), the addition of a methyl group
65 to the C5 position of the cytosine within a cytosine-guanine (CpG) dinucleotide, is the
66 most widely investigated in epidemiological settings due to its relative stability with

67 storage and the multitude of technical platforms available for analysis (Maccani & Marsit,
68 2009).

69 Recently, two genome-wide studies have explored the association between prenatal
70 exposure to green space and DNAm in cord blood. One study, involving 538 neonates
71 from Belgium, identified one significant CpG and 147 DMRs in association with
72 exposure to green space (Alfano et al., 2023). The second study, involving 2,988 mother-
73 infant pairs from seven European birth cohorts, found four DMRs associated with this
74 exposure (Aguilar-Lacasaña et al., 2024). However, to better understand the intrauterine
75 environment, it is crucial to investigate the placenta. This essential organ regulates
76 nutrient and oxygen transfer and hormone and immune supply, and may act as a barrier
77 to environmental exposures, playing a key role in foetal growth and development
78 (Griffiths & Campbell, 2015; Mortillo & Marsit, 2022). To date, only a candidate gene
79 study has explored the association between green space and placental DNAm, where the
80 methylation status of the serotonin receptor *HTR2A* was positively associated with
81 pregnancy green space exposure (Dockx et al., 2022). Thus, it is important to explore the
82 association between maternal green space exposure during pregnancy and DNAm in
83 placenta not only in specific genes but also on a genome-wide scale in relatively large
84 samples sizes. Moreover, the aforementioned studies have mainly relied on residential
85 surrounding greenness and/or proximity to a green space to assess green space exposure,
86 overlooking other important aspects of this complex exposure such as use of green spaces
87 or visual access to green space.

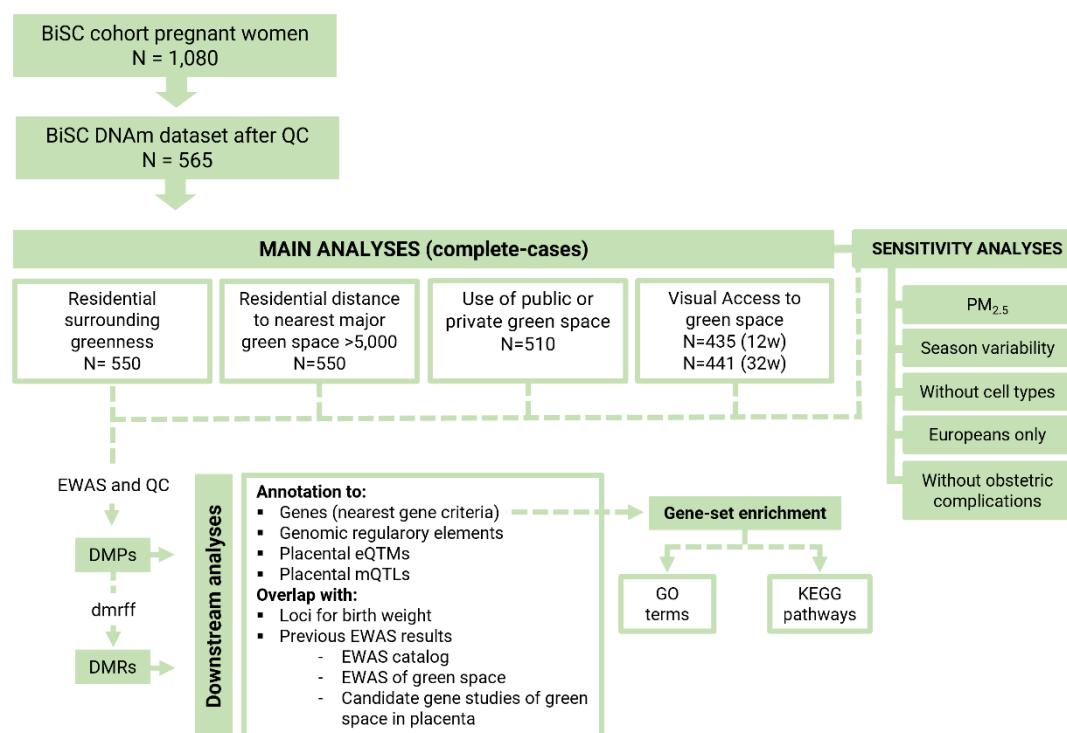
88 Our study aimed to fill these gaps by investigating the association between different
89 aspects of maternal green space exposure during pregnancy and genome-wide placental
90 DNAm. In addition to assessing residential greenness and proximity to green spaces, we

91 also used data on the time spent in green spaces during pregnancy and the visual access
92 to greenery through home windows.

93 **2. Material and methods**

94 *2.1. Study population*

95 The Barcelona Life Study Cohort (BiSC) is a prospective cohort study of 1,080 pregnant
96 women, their offspring and partners in Barcelona that aims to identify early
97 environmental and genetic causes of normal and abnormal growth, development and
98 health from foetal life until young adulthood (Dadvand et al., 2024). Briefly, the
99 enrolment of the BiSC participants was carried out between October 2018 and April 2021
100 at three tertiary university hospitals in Barcelona, Spain. Participants were recruited and
101 had their first data collected at the end of the first trimester of pregnancy, with follow-
102 ups in the second and third trimesters of pregnancy, delivery, and months 1, 2, 6, 8, 12,
103 18, 24, and 48 postnatally. Pregnant women aged 18-45 with singleton pregnancies were
104 included. Exclusions applied to those residing outside the catchment area, not being able
105 to communicate effectively in Spanish, Catalan or English, or with fetuses having known
106 congenital anomalies. The study was approved by the ethical committees of the centers
107 involved in the study, and written informed consent was obtained from all the participants.
108 The detailed description of the recruitment of the study participants, data collection, and
109 follow-ups are reported elsewhere (Dadvand et al., 2024). The total mother-child pairs
110 with data on indicators of green space and placental DNAm included in this study is
111 shown in Figure 1.



112

113 **Figure 1.** Analysis scheme. 12w: week 12 of pregnancy 32w; week 32 of pregnancy; CpG: cytosine-
 114 guanine dinucleotide; DMPs: differentially methylated positions; DMRs: differentially methylated regions;
 115 eQTM: Expression quantitative methylated regions; EWAS: Epigenome-wide association study; GO: Gene
 116 Ontology terms; KEGG: Kyoto Encyclopedia of Genes and Genomes; mQTLs: methylation quantitative
 117 trait loci; QC: quality control; PM_{2.5}: particulate matter with an aerodynamic diameter <2.5 µg/m³; PMD:
 118 partially methylated domains.

119 2.2. Indicators of exposure to green space

120 We characterized four aspects of exposure to green space: (i) residential surrounding
 121 greenness, (ii) residential distance to nearest major green space as a proxy for access to
 122 green spaces, (iii) use of green space, and (iv) visual access to green space through the
 123 home windows.

124 First, to characterize residential surrounding greenness, Normalized Difference
 125 Vegetation Index (NDVI) based on high-resolution (1m x 1m) aerial images (2020)
 126 prepared by Cartographic and Geology Institute of Catalonia was used (Cartographic and

127 Geologic Institute of Catalonia, 2021). NDVI was obtained as a ratio between the red (R)
128 and near infrared (NIR) values in traditional fashion: $(NIR-R) / (NIR + R)$. Its values
129 range between -1 and 1, with higher numbers indicating more greenness (Tucker, 1979).
130 For each participant, residential surrounding greenness was assessed as the time-weighted
131 average NDVI in buffers of 100m, 300m and 500m during pregnancy (Gascon et al.,
132 2016). For those participants who moved home during pregnancy, we calculated an
133 average of these values for all residential addresses weighted by the time spent in each
134 address during pregnancy.

135 Second, residential distance to nearest major green space ($>5,000m^2$) was evaluated using
136 the 2018 land use dataset from the Cartographic and Geology Institute of Catalonia
137 (ICGC), which is based on 1m resolution imagery (Cartographic and Geologic Institute
138 of Catalonia, 2018). The land use categories included urban, agricultural and natural green
139 spaces.

140 Third, the use of green space referred to the amount of time (in hours per week) spent in
141 green spaces during the free time in pregnancy. This indicator was self-reported and
142 collected using questionnaires. Information about the first trimester was collected at week
143 12, while data on the second and third trimesters was collected at week 32 of pregnancy.
144 The question was: “*In a typical week, during your current pregnancy, on average, how*
145 *many hours of your free time do you spend in the following green spaces? (i) public parks,*
146 *(ii) forest and other natural green spaces, and (iii) private garden (at home)*”. To
147 calculate the average number of hours per week that women spent in green spaces during
148 pregnancy, we first summed the hours spent per week in various green spaces for each
149 trimester, including public parks, forests, other natural green spaces, and private gardens
150 at home. Then, we computed the average across the three trimesters. A minimum of data
151 from one trimester was required.

152 Fourth, visual access to green space through the home windows was self-reported and
153 collected using questionnaire at enrolment (week 12 of pregnancy). If they changed
154 homes, mothers were asked to respond this question again at week 32. Given the difficulty
155 of averaging two categorical variables, we examined week 12 (first trimester) and week
156 32 (third trimester) separately. The question was: “*How much greenery (trees, grass,*
157 *flowers, etc) can you see through the living room window? 1 = No greenery/no window;*
158 *2 = A quarter; 3 = Half; 4 = Three quarters; 5 = all is green*”. We dichotomized the
159 answers in: 1 and 2 as visual access to greenery in less than half of the view from the
160 living room, and 3, 4 and 5 as visual access to greenery in equal or more than half of the
161 view from the living room window.

162 *2.3. Placental biopsy and DNA extraction*

163 Out of the 1,080 mother-child pairs that were followed until birth, 611 placentas were
164 collected based on maternal consent and the feasibility of collection at the hospital.
165 Biopsies were obtained by trained gynaecologists following a harmonized protocol across
166 hospitals. Briefly, placenta biopsies of around 2.5 cm (from the maternal to the foetal
167 side) and 1 cm width were obtained from two opposite quadrants at a distance of around
168 3-4 cm from site of cord insertion. Then, these biopsies were cut in two, giving a total of
169 4 biopsies of 2.5 x 0.5 cm. Two of them (one from each quadrant) were directly frozen in
170 liquid nitrogen and transferred to -80C. The other two biopsies were treated with
171 RNAlater and sent to the laboratory where they were divided in four pieces of 0.5 x 0.5
172 cm, corresponding roughly to the foetal membranes, the upper foetal villi, the lower foetal
173 villi and the maternal decidua. Finally, all the biopsies were stored at -80°C for future use.
174 Before DNA extraction, placenta samples were completely randomized and the
175 distribution of main design and biological variables was checked among batches. For
176 genomic DNA extraction, a fragment of approximately 5-6 cm³ (30-40 mg) was dissected

177 from the foetal villi biopsy below the foetal membranes collected in RNAlater. All the
178 dissection process was done in liquid nitrogen to avoid that the tissue was thawed. Then,
179 the tissue was disrupted/homogenized using a bead mill (bead beater) at 4C for 26
180 seconds. Genomic DNA was then isolated using the AllPrep®DNA/RNA/miRNA
181 Universal Kit, (Qiagen, CA, USA). DNA was eluted in 80 ul and stored in different
182 aliquots at -80C. DNA quality was evaluated on a NanoDrop spectrophotometer (Thermo
183 Scientific, Waltham, MA, USA) and additionally 500 ng of DNA was run on 1% agarose
184 gels to confirm that samples did not present visual signs of degradation.

185 *2.4. Methylation data acquisition, quality control and normalization*

186 DNAm assessed in 624 placental DNA samples (including 35 duplicates – 589 unique
187 individuals) with the Infinium MethylationEPIC BeadChip from Illumina, following
188 manufacturer's protocol in the Human Genome facility (HUGE-F) at the Erasmus
189 Medical Centre core facility. Briefly, 750 ng of DNA were bisulfite-converted using the
190 EZ 96-DNAm kit following the manufacturer's standard protocol, and DNAm measured
191 using the Infinium protocol.

192 The methylation data was pre-processed using the PACEAnalysis R package (v.0.1.9)
193 (<https://www.epicenteredresearch.com/>). The pre-processing pipeline consists of probe
194 quality control, sample quality control, normalization, batch correction, winsorization of
195 outlier values and estimation of cell type proportions. Detection p-values were estimated
196 using out-of-band array hybridization as implemented in the SeSAmE R package (Zhou
197 et al., 2018). Probe values were masked if the intensity values were zero, estimated based
198 on less than three beads, and/or if they had a detection p-value>0.05. Based on these
199 criteria (probe call rate <95%), we flagged probes that failed among at least 5% of
200 samples for removal prior to downstream analysis (N= 63,158). Then, fifty-nine samples
201 corresponding to 24 individuals were discarded according to: low methylated and

202 unmethylated signal intensities overall (N=5), sample call rate < 95% (N=3), sex
203 inconsistencies (N=9), samples with indication of substantial contamination with
204 maternal DNA or with DNA from another participant in the study (N=11) (Heiss & Just,
205 2018), duplicates identified by clustering samples based on their genetic similarity using
206 the single nucleotide polymorphisms (SNPs) included in the array (N=29) and siblings
207 (N=2). Exclusion of one of the duplicate pairs was done randomly. A total of 565 samples
208 remained after the sample quality control.

209 After removal of problematic samples, we performed pre-processing of the remaining
210 arrays. Signal intensities were pre-processed by performing linear dye bias correction
211 followed by single-sample background correction based on Normal-exponential
212 convolution using out-of-band Infinium I probes (ssNoob) (J.-P. Fortin et al., 2017;
213 Triche et al., 2013). Unwanted between-array variation was minimized by applying
214 functional normalization using the control probes (J. P. Fortin et al., 2014). Beta-mixture
215 quantile (BMIQ) normalization was then used to correct for the bias of Type-2 probe
216 values (Teschendorff et al., 2013). After that, we explored the clustering of the data
217 through Principal Component Analysis (PCA) and tested the association of the 12 first
218 PCs with main variables (hospital, sex, ethnic origin, birth before or during SARS-CoV-
219 2 pandemic, maternal education and maternal smoking during pregnancy) and technical
220 variables (plate, array, extraction batch, time to placental storage, DNA concentration,
221 and 260/280 and 260/230 ratios) to identify main batch variables. Subsequently, array
222 batch effect was controlled with the ComBat method with the sva Bioconductor R
223 package (Johnson et al., 2007). Following these pre-processing steps, we removed the
224 probes flagged as problematic among the study population. Finally, to correct for the
225 possible outliers, we winsorized the extreme values to the 1% percentile (0.5% in each
226 side), where percentiles were estimated with the empirical beta-distribution. DNAm

227 values are expressed as beta values, where 0 means un-methylation and 1 complete
228 methylation.

229 Cell type proportions of six main placenta populations (trophoblasts, syncytiotrophoblast,
230 nucleated red blood cell, Hofbauer cells, endothelial cells, and stromal cells) were
231 estimated from DNAm using the reference panel from term placentas implemented in the
232 planet R package (V. Yuan et al., 2021).

233 2.5. Covariates

234 The following covariates were selected *a priori* and included in the models: maternal age
235 at recruitment (years), maternal education (no university/university), annual average
236 household income at census tract level as a proxy of neighbourhood socioeconomic status
237 (SES) (euros), child ethnicity (European/Latino-American/other), maternal smoking
238 during pregnancy (no/yes), child sex (female/male), gestational age at birth (weeks),
239 parity (nulliparous/ multiparous), hospital of birth, COVID19 confinement, which
240 indicates whether any part of the pregnancy took place during the confinement and was
241 categorized in three levels: pre-confinement (the whole pregnancy took place before
242 confinement / confinement (part of the pregnancy took place during confinement) and
243 post-confinement (the whole pregnancy took place after confinement), DNA
244 contamination score and placental cell type proportions. Data on maternal age, maternal
245 education, child ethnicity, maternal smoking during pregnancy and parity were self-
246 reported and collected using a questionnaire at enrolment (week 12 of pregnancy). Annual
247 average household income at census tract level obtained from the 2020 Standard of Living
248 and Living Conditions survey conducted by the Spanish National Institute of Statistics
249 (INE), which is based on fiscal data including wages, pensions, unemployment benefits,
250 other benefits, and other income (Spanish National Institute of Statistics, 2023). Child sex
251 was retrieved from clinical records. Gestational age at birth was calculated from the date

252 of the last menstrual period using estimates based on the first ultrasound examination
253 (about 12th week of gestation). DNA contamination score was calculated as the average
254 log odds from the SNP posterior probabilities from the outlier component; capturing how
255 irregular the SNP beta-values deviate from the ideal trimodal distribution (Heiss & Just,
256 2018).

257 *2.6. Statistical analyses*

258 *2.6.1. Differentially methylated positions (DMPs)*

259 Epigenome-wide association studies (EWAS) using robust linear regression models were
260 fitted to evaluate the association between maternal exposure to green space during
261 pregnancy (predictor) and placental DNAm (outcome) using the PACEanalysis R
262 package (<https://github.com/epicenteredresearch/PACEanalysis>). Main models were
263 adjusted for the covariates described above.

264 We performed the quality control of the EWAS results for each model using the EASIER
265 R package (*ISGlobal-Brge/EASIER: Tools for Methylation Data Analysis*, 2022) (Table
266 S2). This included examining inflation and the distribution of effect estimates, standard
267 errors and p-values. We excluded control probes, non-CpG probes, probes that mapped
268 to X/Y chromosomes, probes with poor base pairing quality (lower than 40 on 0-60 scale),
269 probes with non-unique 30bp 3'-subsequence (with cross-hybridizing problems),
270 Infinium II probes with SNPs of global minor allele frequency (MAF) over 1% affecting
271 the extension base, probes with a SNP in the extension base that causes a color channel
272 switch from the official annotation (Zhou et al., 2017) and probes that have shown to be
273 unreliable in a recent comparison of the Illumina 450K and EPIC BeadChips (Fernandez-
274 Jimenez et al., 2019). The percentage of probes removed was 13.98% (Appendix A: Table
275 S2).

276 Continuous green space indicators (residential surrounding greenness, residential
277 distance to nearest major green space and use of green space) were standardized by
278 dividing them by its interquartile range (IQR). Effect sizes are reported as the difference
279 in DNA m unit by IQR of continuous exposures, or by exposure group of the categorical
280 variables. Multiple testing was accounted for by applying Bonferroni correction (BN) for
281 694,380 tests (P-value $<7.2 \times 10^{-8}$). Significance was considered suggestive for p-values
282 $<1 \times 10^{-5}$.

283 2.6.2. *Differentially methylated regions (DMRs)*

284 DMRs were identified using the *dmrff* R package (Suderman et al., 2018). This method
285 identifies candidate DMRs by screening the EWAS results for genomic regions each
286 covered by a sequence of CpG sites with effects in the same direction, p-values <0.05 ,
287 and <500 bp gaps between consecutive CpG sites. We considered statistically significant
288 DMRs those detected with a BN p-value <0.05 and with a minimum of three consecutive
289 CpGs within the DMR.

290 2.6.3. *Sensitivity analyses*

291 Five sensitivity analyses were conducted by repeating the DMP and DMR analyses: i)
292 additionally adjusting for the average exposure to particulate matter with an aerodynamic
293 diameter $<2.5 \mu\text{g}/\text{m}^3$ (PM_{2.5}) as a proxy of air pollution during pregnancy ii) additionally
294 adjusting for season of conception to investigate seasonal variability; iii) without
295 adjusting for cell type proportions; iv) restricted to European ethnicity only, which was
296 the largest ethnic subgroup, and v) excluding obstetric complications (preterm births,
297 foetus with growth restriction and pregnancy complications related to the placenta: pre-
298 eclampsia/eclampsia, gestational hypertension, placental abruption, placenta previa,
299 oligohydramnios, polyhydramnios and chorioamnionitis).

300 We assessed maternal exposure to particulate matter with an aerodynamic diameter < 2.5
301 μm ($\text{PM}_{2.5}$) using land use regression (LUR) models using the environmental data around
302 collected in the BISC campaigns, following the guidelines established by the European
303 Study of Cohorts for Air Pollution Effects (ESCAPE) (Dadvand et al., 2024). The
304 measurement calculated around the addresses of mothers' homes was used to adjust the
305 model of the residential green space indicators (surrounding greenness, distance and
306 visual access), while the measurement considering all environments (home, workplace,
307 and commuting route) was used to adjust the model of use of green space.
308 Season of conception (autumn / spring / summer / winter) was calculated by subtracting
309 the gestational days of pregnancy (last menstrual period) from the date of birth. Preterm
310 was defined as a gestational age at birth of less than 37 weeks. Foetal growth restriction
311 was defined as a birth weight percentile <3 or a birth weight percentile <10 and
312 cerebroplacental ratio pulsatility index percentile at 32w <5 or a birth weight percentile
313 <10 and uterine artery pulsatility index percentile at 32w >95 . Birth weight percentiles
314 were estimated according to the BCNatal curves (Figueras et al., 2008; Figueras &
315 Gratacós, 2014). Pulsatility indexes were measured through Doppler and percentiles
316 calculated using reference curves described elsewhere (Baschat & Gembruch, 2003;
317 Gómez et al., 2008).

318 **2.7. Downstream analyses**

319 First, we tested the overlap of the BN significant DMPs and DMRs with placental
320 chromatin states (Ernst & Kellis, 2017), placenta germline differently methylated regions
321 (gDMRs) (Hamada et al., 2016), and placenta partially methylated domains (PMDs)
322 (Schroeder et al., 2013). Second, to assess whether the methylation levels of the DMP
323 and DMRs were associated with the expression levels of nearby genes, we examined
324 previously identified Expression Quantitative Trait Methylation (eQTM) in the placenta

325 (Delahaye et al., 2018; Deyssenroth et al., 2020). Third, we checked whether the BN
326 significant DMPs and CpGs within the significant DMRs had previously been associated
327 with exposures or health traits using the information from the EWAS Catalog (Battram,
328 Yousefi, et al., 2022). (Battram, Yousefi, et al., 2022). Fourth, we compared the list of
329 BN significant DMPs and DMRs with previously reported studies investigating the
330 association between exposure to green space during pregnancy and DNAm in cord blood
331 (Aguilar-Lacasaña et al., 2024; Alfano et al., 2023) and a candidate gene study in placenta
332 (Dockx et al., 2022).

333 As DNAm is partially regulated by genetic variants, we explored whether the DMP and
334 CpGs in the DMRs found in our study had any methylation Quantitative Trait Loci
335 (mQTLs). Foetal cis mQTLs (± 0.5 Mb, 1 Mb window) were identified in the BiSC study
336 ($n=408$) by applying a linear regression for each CpG-SNP pair adjusting for child's sex,
337 child's gestational age at birth, child's ancestry based on 5 genetic principal components
338 (PCs), 6 placental cell type proportions estimated from DNA methylation data using the
339 TensorQTL tool (Ongen et al., 2016). Genome-wide significance was established at 5×10^{-8} .
340 Placental DNAm was measured with the EPIC array as described above, and foetal
341 genome-wide genotyping (placenta or cord blood) was conducted using the Infinium
342 Global Screening (GSA) array v.3.0 array and imputed with the Haplotype Reference
343 Consortium (HRC) panel.

344 Additionally, we assessed the overlap with genomic regions of previously identified SNPs
345 for birth weight in the largest genome-wide association study (GWAS) to date
346 (Juliusdottir et al., 2021). The overlap was investigated using the the GenomicRanges R
347 package (Lawrence et al., 2013) and by defining 1 Mb windows (± 0.5 Mb) surrounding
348 each of the autosomal SNPs identified in the GWAS.

349 Then, the DMP and DMRs were annotated to genes using the Illumina's annotation file,
350 which annotates CpGs located within a distance of 1500bp from the transcription start
351 site (TSS). If the CpG did not have a gene annotated within this distance, then the
352 University of California, Santa Cruz (UCSC) Genome Browser was referenced to identify
353 the nearest gene using the matchGenes() function from the bumpHunter R package (Jaffe
354 et al., 2012). We conducted functional enrichment analyses for Gene Ontology (GO)
355 terms (Kanehisa, 2000) and pathways of the Kyoto Encyclopedia of Genes and Genomes
356 (KEGG) (Kanehisa, 2000) of genes annotated to the suggestive DMPs (p -value $< 1 \times 10^{-5}$)
357 and CpGs within the BN significant DMRs, using the missMethyl method (Phipson et al.,
358 2016) as implemented in EASIER R package (ISGlobal-Brge/EASIER: Tools for
359 Methylation Data Analysis, 2022).

360 **3. Results**

361 *3.1. Study population*

362 A total of 550 participants were included in the study. A detailed description of our study
363 population characteristics is presented in Table 1; Appendix A: Table S1. The median age
364 of the mothers was 34.4 years old, around two thirds had university education and 7.0%
365 smoked during pregnancy. The median gestational age at birth was 40.0 weeks, half of
366 the offspring were girls, 67.5% of them were Europeans, 28.9% Latino-American, and
367 the rest from other ethnicities. Median residential NDVI value was 0.2, the median
368 residential distance to a green space was 129.9 m and a median of 3 h per week were
369 spent in public and/or private green spaces. Furthermore, around one-third of the mothers
370 had visual access to greenery in more than half of the living room window during the first
371 and third trimesters. The correlation coefficients across the different indicators of
372 residential surrounding greenness (NDVI 100m, 300m and 500m) were high, especially
373 between the 300m and 500m buffers. For visual access, the correlation between the first

374 and third trimesters was also very high. We found inverse moderate correlations across
 375 residential surrounding greenness and residential distance to a major green space. The
 376 correlation coefficients across all green space exposures are shown in Appendix B: Figure
 377 S1.

Table 1. Characteristics of the BiSC study population (N= 550)

	Median (IQR) / n (%)
<i>Pregnancy green space indicators</i>	
Residential greenness	
NDVI 100m buffer	0.21 (0.18 - 0.24)
NDVI 300m buffer	0.22 (0.19 - 0.24)
NDVI 500m buffer	0.22 (0.20 - 0.25)
Residential distance to nearest major green space >5,000 (meters)	129.90 (63.22 - 227.94)
Use of public and private green space (hours/week) (n missing = 47)	3.17 (1.00 - 6.33)
Visual access to greenery through living room window	
First trimester (12w) (n missing = 115)	
Less than half	288 (66.21)
Half or more	147 (33.79)
Third trimester (32w) (n missing = 109)	
Less than half	285 (64.63)
Half or more	156 (35.37)
<i>Maternal characteristics</i>	
Maternal age (years)	34.38 (31.25 - 37.74)
Maternal education	
No university	183 (33.27)
University	367 (66.73)
Maternal smoking during pregnancy	
No	511 (92.91)
Yes	39 (7.09)
<i>Child characteristics</i>	
Child sex	
Girls	273 (49.64)
Boys	277 (50.36)
Child ethnicity	
European	371 (67.45)
Latino-American	159 (28.91)
Other	20 (3.64)

12w: week 12 of pregnancy 32w; week 32 of pregnancy; NDVI: satellite-based Normalized Difference Vegetation Index; PM_{2.5}: Particulate matter with aerodynamic diameter <2.5µm.

378

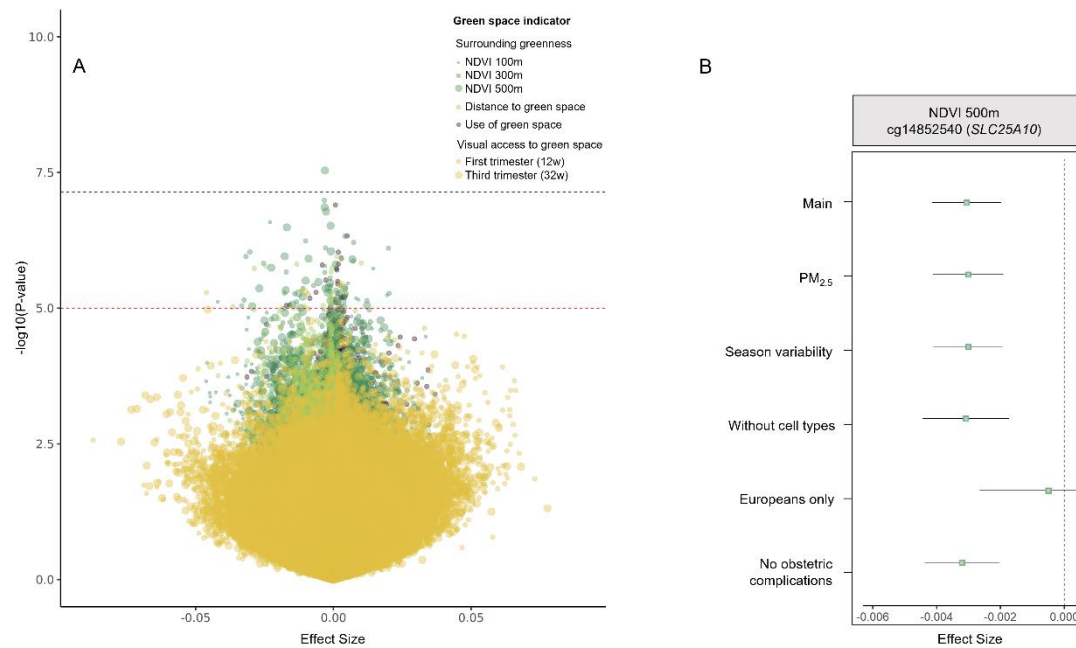
379

380 3.2. *Green space during pregnancy and placental DNAm*

381 3.2.1. *DMPs*

382 The lambda inflation factors for the main models ranged from 0.84 to 1.26 (Appendix A:
383 Table S2; Appendix B: Figure S2). After BN correction, one DMP (cg14852540)
384 annotated to the *SLC25A10* gene was significantly associated with residential surrounding
385 greenness in 500m buffer. At this DMP, for an IQR increase of NDVI in 500m, DNAm
386 was 0.3% lower. The effect at this site remained consistent in both the 100m and 300m
387 buffers, although not statistically significant (Appendix A: Table S3). No DMPs were
388 significantly associated with residential distance, use or visual access to green space. At
389 suggestive significance ($p\text{-value} < 1 \times 10^{-5}$), 101 unique DMPs were associated with at least
390 one green space indicator (Figure 2A; Appendix A: Table S3). Pearson correlation
391 coefficients of the effect estimates of all genome-wide CpGs and the BN DMP across the
392 EWAS results from the green space indicators are shown in Appendix A: Table S4;
393 Appendix B: Figure S3.

394 In terms of sensitivity analyses, the most notable difference in effect size among the BN
395 significant DMP was observed when we restricted the analyses to Europeans ($n=371$),
396 leading to an 83.6% decrease in the effect estimate (Figure 2B). Effect sizes did not
397 change substantially in the rest of sensitivity analyses. The percentage differences in
398 absolute values in the effects between the main and the sensitivity results were as follows:
399 a decrease of 1.6% for $PM_{2.5}$ adjustment, a decrease of 1.5% for season of conception
400 adjustment, an increase of 0.6% for cell type proportion unadjusted model and an increase
401 of 5.5% when excluding obstetric complications (Figure 2B; Appendix A: Table S5).



402

403 **Fig 2.** (A) Volcano plot showing the effect sizes on the x-axis and the (-log₁₀) p-values on the y-axis for the
 404 association between all pregnancy green space indicators and placental DNAm. Each dot represents the
 405 association of one CpG with one exposure variable. The color of the dot indicates the exposure: Surrounding
 406 greenness (dark green), distance to green space (light green), use of green space (purple) and visual access
 407 to green space (yellow). Dot sizes correspond to the sizes of the NDVI buffers and time window of visual
 408 access (week 12 and week 32 of pregnancy). The black line represents the BN p-value threshold (7.2×10^{-8})
 409 and the red line represents the suggestive p-value (1×10^{-5}). (B) Forest plot showing the effect size and 95%
 410 confidence interval of the BN significant DMP in the main model compared with the sensitivity analyses:
 411 1) adjusted for PM_{2.5} during pregnancy; 2) adjusted for season of conception; 3) without adjusting for cell
 412 type proportions; 4) restricted to European ethnicity, and 5) without obstetric complications (preterm births,
 413 cases of FGR and pregnancy complications).

414 3.2.2. DMRs

415 Ten unique DMRs, annotated to 10 genes, were associated with pregnancy exposure to
 416 different green space indicators after BN correction. Residential surrounding greenness
 417 in 500m was associated with four DMRs, two of which were also associated with 300m
 418 buffer. Distance to green space was associated to five DMRs and visual access to green
 419 space during the first trimester was inversely associated with one DMR. This DMR,
 420 associated with visual access during the first trimester, was no longer identified with this

421 exposure in the third trimester. However, an overlapping DMR was detected with nominal
422 significance ($p\text{-value} = 2.77 \times 10^{-5}$) (Appendix A: Table S6). These DMRs included from
423 three to eight CpGs with widths ranging from 20 to 382 bp. No DMPs were significantly
424 associated with residential surrounding greenness in 100m, use of green space or visual
425 access to green space during the third trimester. More detailed information on each DMR
426 is provided in Table 2. Additionally, the genes annotated to the significant DMRs that
427 overlap across the evaluated green space indicators are shown in Figure 3.

428 In the sensitivity analyses, the smallest difference in the number of significant DMRs was
429 observed after adjusting for the season of conception, with 9 out of 10 DMRs remaining
430 significant. In contrast, the largest difference in the number of significant DMRs was seen
431 when restricting the analysis to Europeans only, detecting 4 out of the 10 significant
432 DMRs from the main model. The absolute percentage differences in effect across the
433 main and sensitivity results for DMRs that remained significant varied as follows: 0.4%
434 to 2.67% for $PM_{2.5}$ adjustment, 0.8% to 8.1% for season of conception adjustment, 0.3%
435 to 24.1% for unadjusted cellular composition, 11.3% to 22.6% when restricted to
436 Europeans only, and 1.7% to 14.2% for the model excluding obstetric complications
437 (Appendix A: Table S7).

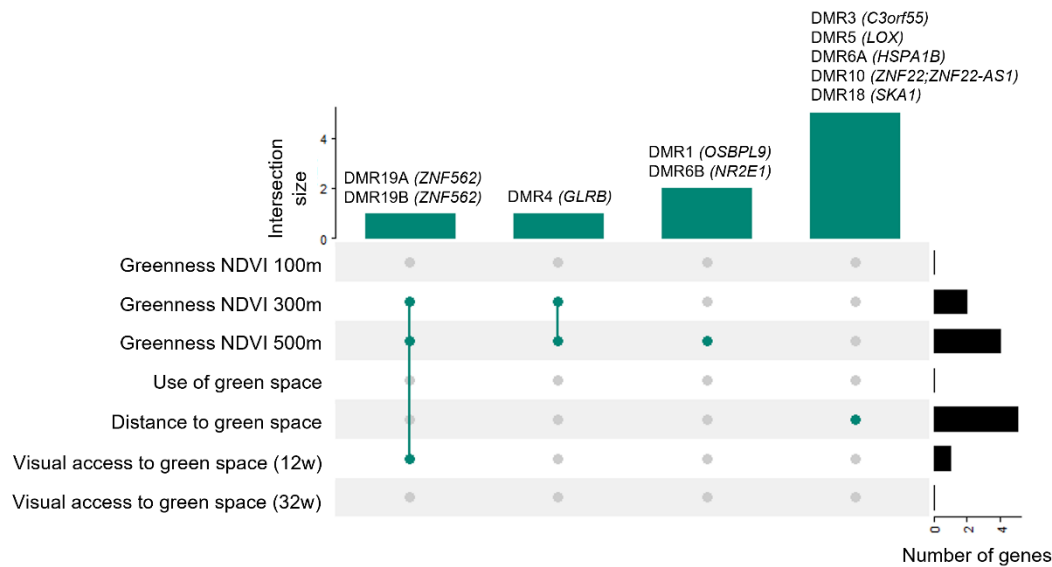
Table 2. Differentially methylated regions (DMRs) associated with green space indicators in placenta

Green space indicator	DMR name	Genomic location (GRCh37/hg19)	Width (bp)	N CpGs	Coefficient ^a	SE	P-value	BN	Gene ^b	Region	Distance 5' extreme	Gene length
NDVI 300m	DMR4	chr4:157997360-157997554	194	6	-0.0132	0.0021	1.28E-10	9.54E-05	<i>GLRB</i>	promoter	1	95687
	DMR19B	chr19:9785779-9786131	352	8	0.0084	0.0010	5.88E-18	4.37E-12	<i>ZNF562</i>	promoter	3	22387
NDVI 500m	DMR1	chr1:52195423-52195670	247	3	0.0068	0.0012	6.10E-08	4.53E-02	<i>OSBPL9</i>	overlaps 5'	0	59405
	DMR4	chr4:157997360-157997554	194	6	-0.0126	0.0020	1.47E-10	1.09E-04	<i>GLRB</i>	promoter	1	95687
	DMR6B	chr6:108479243-108479557	314	4	0.0146	0.0024	2.07E-09	1.54E-03	<i>NR2E1</i>	upstream	7658	22798
	DMR19B	chr19:9785779-9786131	352	8	0.0078	0.0008	3.20E-21	2.38E-15	<i>ZNF562</i>	promoter	3	22387
Distance to green space	DMR3	chr3:157261086-157261106	20	3	-0.0353	0.0049	6.67E-13	5.15E-07	<i>C3orf55</i>	promoter	27	57888
	DMR5	chr5:121413797-121414029	232	3	-0.0411	0.0059	4.25E-12	3.28E-06	<i>LOX</i>	inside	26	15165
	DMR6A	chr6:31795195-31795573	378	3	-0.0093	0.0016	6.02E-09	4.65E-03	<i>HSPA1B</i>	overlaps 5'	0	2519
	DMR10	chr10:45496482-45496710	228	4	-0.0147	0.0027	4.69E-08	3.62E-02	<i>ZNF22;</i> <i>ZNF22-AS1</i>	promoter	12	3324
	DMR18	chr18:47901210-47901419	209	5	-0.0051	0.0008	1.73E-11	1.33E-05	<i>SKA1</i>	overlaps 5'	0	19146
Visual access (12w)	DMR19A	chr19:9785647-9786029	382	8	-0.0134	0.0019	1.42E-12	1.03E-06	<i>ZNF562</i>	overlaps 5'	0	22387

Only those DMRs detected with Bonferroni-adjusted P-value < 0.05 and with three consecutive CpGs within the DMR were considered. DMR name: name of the DMR. The number corresponds to the chromosome where it is located. If there are multiple DMRs on the same chromosome, they are named alphabetically (e.g., On chromosome 1, there are two DMRs named as DMR1A and DMR1B). Genomic location: refers to Genome Research Consortium human genome build 37 (GRCh37)/UCSC human genome 19 (hg19); Width: width of the region (difference between the end and the start position of the DMR); N CpGs: number of CpGs included in the DMR; SE: standard error; P-value: nominal P-value; BN: bonferroni-adjusted P-value; Region: region where the DMR is located in relation to the gene. Distance 5' extreme: distance from the DMR to the 5' end of the gene; Gene length: length of the gene; 12w: week 12 of pregnancy (first trimester).

^a The regression coefficients are reported as the difference in DNA methylation in the whole DMR by IQR of continuous exposures to green space (NDVI 100m, NDVI 300m, NDVI 500, Distance to green space and Use of green space) or by exposure group of the categorical variables (Visual access to green space) (ie. visual access to greenery equal to or more than half of the living room window vs. less than half).

^b DMRs were annotated to genes using the Illumina's annotation file, which annotates CpGs within a distance of 1500 bp from the transcription start site (TSS) of the gene. If the DMR did not have a gene annotated within a distance of 1500 bp from the promoter region of the gene distance, then the University of California, Santa Cruz (UCSC) Genome Browser was referenced to identify the nearest gene using the matchGenes() function from the bumpHunter package.



439

440 **Fig. 3.** Upset plot representing the complete or partial overlap of significant DMRs across the different
 441 green space indicators. The dots indicate the presence (green) or absence (grey) of DMRs overlapping
 442 across the exposure categories. The green bars indicate the number of DMRs that overlap across the green
 443 space indicators. The black bars on the right indicate the total number of genes annotated to a DMR for
 444 each green space indicator. 12w: week 12 of pregnancy; 32w: week 32 of pregnancy.

445 3.3.3. Downstream analyses

446 We searched whether the BN significant DMP and DMRs (42 CpG sites in total) were
 447 located in specific genomic regulatory elements of the placenta. More than 80% (34/42)
 448 were located in active regions: active TSS (TssA), flanking active TSS (TssAFlink) and
 449 enhancers (Enh). Moreover, DMR18 (chr18:47901210-47901419) overlapped with two
 450 placental PMDs, regions known to contain relevant genes for placental function
 451 (Schroeder et al., 2013). However, none of the DMP or DMRs overlapped with placental
 452 gDMRs (Appendix A: Table S8). Regarding gene expression, none of the significant
 453 DMP or DMRs overlapped with the eQTM identified in the placenta (Appendix A: Table
 454 S8). According to genetic variation, the DMP (cg14852540) and one DMR (DMR3) were
 455 close to two fetal SNPs associated with birth weight (rs73354194 and rs13322435)
 456 (Juliusdottir et al., 2021). However, neither of these CpGs has a cis-mQTL in placenta
 457 (Appendix A: Table S8).

458 As one BN significant DMP was not enough to perform a gene-set enrichment analyses,
459 we included those DMPs associated to a green space indicator at the suggestive threshold
460 (p -value $< 1 \times 10^{-5}$) and CpGs within the BN DMRs. Although not significant after multiple
461 testing correction, among the top pathways where these genes were involved,
462 glucocorticoid synthesis and secretion (cortisol), inflammatory response, regulation of
463 response to reactive oxygen species, and longevity regulating pathways, were among the
464 top ones (nominal p -value < 0.1) (Appendix A: Table S9-S10).

465 Neither the DMP nor the DMRs found in this study overlapped with previous findings or
466 vice versa when evaluating the association between green space exposure and DNAm in
467 cord blood (Aguilar-Lacasaña et al., 2024; Alfano et al., 2023) or in placenta (Dockx et
468 al., 2022) (Appendix X: Table S11).

469 According to the EWAS Catalog, methylation levels at the significant DMP or CpGs
470 within the significant DMRs have previously been related to child age, gestational age,
471 autoimmune diseases such as rheumatoid arthritis and respiratory conditions such as
472 chronic obstructive pulmonary disease (COPD). None of these studies were conducted in
473 placenta and most of them evaluated in blood (see Appendix A: Table S8 for detailed
474 information).

475 **4. Discussion**

476 This study evaluated association of different aspects of maternal exposure to green space
477 during pregnancy and placental DNAm in the BiSC cohort. We found that this exposure
478 was associated with one DMP (cg14852540 annotated to *SLC25A10* gene) and 10 unique
479 DMRs.

480 The DMP that we identified in relation to residential greenness within 500m buffer was
481 annotated to the gene body of the *Solute carrier family 25 member 10 (SLC25A10)*.
482 *SLC25A10*, a dicarboxylate carrier, plays a role in metabolic processes by transporting

483 small molecules into or out of the mitochondria thereby providing substrates for
484 metabolic processes including the Krebs cycle and fatty acid synthesis (Freund et al.,
485 2014; Huypens et al., 2011; Mizuarai et al., 2005). Buccal mitochondria DNA content
486 (mtDNAC), a proxy of mitochondrial function (Castellani et al., 2020), has been positively
487 associated with green space exposure (Hautekiet et al., 2022). Furthermore, mitochondrial
488 respiration has been shown to play a role in the invasive and migratory capabilities of
489 trophoblasts, which are necessary for embryo implantation and placental development
490 (Xiong et al., 2024; Yu et al., 2024). Additionally, recent studies found that DNAm of
491 this gene in blood was associated with body mass index and waist circumference in
492 adolescents (Huang et al., 2022). Finally, this DMP was located at <0.5 Mb of a loci
493 containing foetal SNPs associated with birth weight (Juliusdottir et al., 2021), which may
494 suggest the involvement of this genomic region in foetal growth.

495 Besides this DMP, we also identified 10 DMRs. Two of them (DMR19A and DMR19B)
496 were associated with residential greenness and visual access to green space, respectively.
497 These DMRs partially overlapped in the promoter region of *the Zinc Finger Protein 562*
498 (*ZNF562*) gene. Despite being in the same region, these DMRs showed opposite effects.
499 The reason for these differences is unclear, and further investigation is needed. Moreover,
500 we observe that DMR19B, which was associated with visual access during the first
501 trimester, did not remain significant after multiple testing in the third trimester. However,
502 an overlapping DMR was detected with nominal significance, and with the same direction
503 of effect. This gene may be involved in transcriptional regulation, and a recent study
504 suggests that it might be related to glutamine metabolism its involvement in glutamine
505 metabolism (Shi et al., 2024), an amino-acid essential for foetal growth, especially in later
506 gestation (Wu et al., 2015). In a previous study, a placental DMR (chr19:9785647-

507 9785919) covering this gene and overlapping our DMRs was linked to a "vegetarian
508 tendency" pattern (Lecorguillé et al., 2022).

509 Additionally, we found that residential surrounding greenness was associated with two
510 other DMRs (DMR1, DMR4) annotated to *OSBPL9* and *GLRB*, respectively. First,
511 DMR1 overlapped the 5' untranslated region (5'UTR) of the *Oxysterol Binding Protein*
512 *Like 9 (OSBPL9)* gene, known for its role in lipid metabolism (Paterson et al., 2022).
513 Second, DMR4 located in the promoter of the *Glycine Receptor Beta (GLRB)* gene was
514 inversely associated with residential surrounding greenness within 300m and 500m
515 buffer. *GLRB* encodes the beta subunit of glycine receptors, which are neurotransmitter-
516 gated ion channels found throughout the central nervous system, including the
517 hippocampus, spinal cord, and brain stem (Handford et al., 1996). This gene has been
518 associated with neurological disorders such as hyperekplexia (L. Zhou et al., 2002).

519 Distance to green space was also associated to DMRs located inside or near the promoter
520 of the following genes: *Solute Carrier Family 66 Member 1 Like, Pseudogene (C3orf55)*
521 participating in L-lysine transport and close to a SNP associated with birth weight
522 (Juliusdottir et al., 2021); *Lysile Oxidase (LOX)* involved in collagen and elastin cross-
523 linking (Guo et al., 2016); *Spindle And Kinetochore Associated Complex Subunit 1*
524 (*SKA1*), crucial for proper chromosome segregation (Welburn et al., 2009); *Heat Shock*
525 *Protein Family A (Hsp70) Member 1B (HSPA1B)*, playing a role in placenta-derived stem
526 cells in the heat-induced proteotoxic stress response, which is crucial for protecting the
527 proteome against stress (Alharbi et al., 2022); and Zinc Finger Protein family genes such
528 as *Zinc Finger Protein 22 (ZNF22)* and *ZNF22 Antisense RNA 1 (ZNF22-AS1)*, may be
529 involved in transcriptional regulation (Paterson et al., 2022), although limited findings in
530 relation to these genes have been published so far.

531 Among the top gene-sets and GO and KEGG terms identified, although not surviving
532 multiple-testing, there were glucocorticoid related pathways, longevity regulating
533 pathway, inflammatory response, and regulation of response to reactive oxygen species.
534 The genes in the glucocorticoid-related pathways whose DNAm levels were suggestively
535 associated with green spaces in our study were *Adenylate Cyclase 4 (ADCY4)*, *Aryl*
536 *Hydrocarbon Receptor Interacting Protein (AIP)* and *Phosphodiesterase 8A (PDE8A)*
537 genes. Glucocorticoids have a central role in foetal maturation, but excessive levels can
538 induce foetal growth restriction (Fowden et al., 2016). According to the literature, stress
539 reduction could be one of the mechanisms linking green exposure to improved health
540 outcomes through epigenetics (Nwanaji-Enwerem et al., 2024). Moreover, in a previous
541 study, higher residential surrounding greenness, residential proximity to green spaces,
542 longer time spent in green spaces, and more visual access to green space during pregnancy
543 were associated with lower cortisol level in cord blood (Boll et al., 2020). Therefore,
544 larger studies with increased statistical power are needed to explore this pathway
545 concerning green space and its potential implications for placental and foetal
546 development.

547 To date, two recent studies evaluated the association between residential greenness
548 exposure during the prenatal period, a critical period for perinatal and life-long health,
549 with DNAm in cord blood (Aguilar-Lacasaña et al., 2024; Alfano et al., 2023). None of
550 the DMP or DMRs identified in this study overlapped with the findings from the
551 aforementioned studies. This could be explained by the differences between tissues
552 (Ohgane et al., 2008), but also differences in the exposure and outcome assessment.

553 Alfano et al., used land cover data to classify green space based on vegetation height,
554 rather than NDVI, to calculate green space exposure. Additionally, the buffer of 100m
555 was the only one common to both studies. In our analysis, we did not observe any

556 significant DMP or DMR within this buffer. Moreover, the lack of overlap with our
557 previous study (Aguilar-Lacasaña et al.,) may be due to the different resolutions of the
558 aerial images used, with the current study having a much higher resolution (1m x 1m)
559 compared to the previous study (30 x 30m).

560 In placenta, only a candidate gene study (N=327) has explored the association between
561 green space and DNAm (Dockx et al., 2022). In that study, methylation levels at the
562 promoter of *5-Hydroxytryptamine Receptor 2A (HTR2A)* gene, a serotonin receptor with
563 a potential effect on neurodevelopment function, was positively associated with maternal
564 green space exposure within 1,000 m, 2,000 m and 3,000 m buffers measured using land
565 cover data and stratified into low (<3 m) and high (≥ 3 m) vegetation. We were unable to
566 assess the same CpGs in our study as they were not included in the EPIC array. Therefore,
567 we examined the direction of the effect of nearby CpGs located in the promoter region
568 (cg27068143 and cg10323433) of *HTR2A*, and although not statistically significant
569 (nominal P-value >0.05), they showed a consistent direction of the effect in our study.

570 One of the strengths of this study was the analysis of a relatively large number of placental
571 samples, a relevant tissue for foetal development. Second, to characterize residential
572 surrounding greenness, NDVI was derived from high-resolution (1x1) aerial images and
573 averaged over the entire pregnancy, considering the changes in participants' residences.
574 Moreover, we expanded our analyses beyond surrounding greenness by including other
575 green space indicators such as distance to nearest major green space, use of green spaces
576 and also visual access to greenery through the home window. Third, DMRs were detected
577 using the *dmrff* R package, considered the gold standard for calculating DMRs (Lent et
578 al., 2021). Fourth, relying on wealth of available data in BiSC, we were able to conducted
579 sensitivity analyses by further adjusting our analyses for air pollution, season of

580 conception, cellular composition or excluding pregnancy and foetal complications, and
581 we observed that our findings were generally robust after conducting these analyses.
582 It is important to interpret the results of this study considering its limitations. First, despite
583 being the largest study on placenta evaluating the association of prenatal exposure to
584 green space and DNAm, our study might have been underpowered for detecting some of
585 the associations. For example, the decrease in the number of significant DMRs observed
586 when restricting the analysis to European ethnicity (N= 371), compared to the main
587 analysis including all ethnicities, may be attributed to the decrease in statistical power
588 due to the reduction in sample size. Also, the effect size of the significant DMP was
589 reduced substantially in the subset of Europeans, suggesting some residual confounding
590 by ethnic origin not well controlled in the full population. We note that models were
591 adjusted for ethnic origin. Larger sample sizes are needed to investigate ethnicity and
592 ancestry specific effects. Moreover, we did not examine sex-specific or cell-interacting
593 associations due to statistical power limitations. Second, we did not have data in other
594 important aspects of the green space exposure, such as type of vegetation and quality
595 characteristics of the green space. Third, the variable measuring the use of green space
596 was obtained from questionnaire, which could have resulted in exposure
597 misclassification. Validating this measure by employing other techniques such as mobile
598 phone Global Positioning System (GPS) data would improve its reliability (Heikinheimo
599 et al., 2020). Fourth, whilst we controlled our analyses for a wide array of covariates, we
600 cannot assume that associations we found are causal. In the same way, we cannot assume
601 that differences in DNAm will affect health outcomes, as epigenetic mechanisms are more
602 complex than what can be discerned from DNAm (Min et al., 2021). Finally, in addition
603 to being unable to explore associations with other epigenetic marks and gene expression,
604 this study, in common with other EWAS studies, covers only a small proportion of the

605 epigenome (less than 5% of the 23 million CpGs for the EPIC array) (Battram et al.,
606 2022).

607 **5. Conclusion**

608 Overall, we identified associations between green space exposure during pregnancy and
609 DNAm levels in placenta at one DMP and ten DMRs annotated to genes involved in
610 transcriptional regulation, metabolic pathways and mitochondrial respiration. This points
611 to a potential role of placental epigenetic mechanisms in the effects of green space
612 exposure during pregnancy on birth outcomes and offspring health. However, further
613 research is needed to validate these results and understand the underlying biological
614 pathways.

615 **CRedit authorship contribution statement**

616 **Sofía Aguilar-Lacasaña:** Conceptualization, Methodology, Formal analysis,
617 Investigation, Resources, Data curation, Writing - Original Draft, Writing - Review &
618 Editing, Visualization. **Marta Cosin-Tomas:** Conceptualization, Methodology,
619 Resources, Writing-review & editing, Supervision. **Bruno Raimbault:** Data curation,
620 Methodology, Writing - Review & Editing. **Laura Gómez:** Resources, Data curation,
621 Writing - Review & Editing. **Olga Sánchez:** Resources, Writing-review & editing.
622 **Maria Julia Zanini:** Resources, Writing-review & editing. **Rosalía Pascal Capdevila:**
623 Resources, Writing-review & editing. **Maria Foraster:** Resources, Writing-review &
624 editing. **Mireia Gascon:** Resources, Writing-review & editing. **Ioar Rivas:** Resources,
625 Writing-review & editing. **Elisa Llurba:** Resources, Writing-review & editing. **Maria**
626 **Dolores Gómez-Roig:** Resources, Writing-review & editing. **Jordi Sunyer:**
627 Conceptualization, Investigation, Writing - Review & Editing, Supervision, Funding
628 acquisition. **Mariona Bustamante:** Conceptualization, Methodology, Investigation,
629 Writing - Review & Editing, Supervision, Funding acquisition. **Martine Vrijheid:**

630 Conceptualization, Investigation, Writing - Review & Editing, Supervision, Funding
631 acquisition. **Payam Dadvand:** Conceptualization, Methodology, Investigation, Writing -
632 Review & Editing, Supervision, Funding acquisition.

633 **Acknowledgments**

634 This work was supported by the European Joint Programming Initiative “A Healthy Diet
635 for a Healthy Life” (JPI HDHL and Instituto de Salud Carlos III) – NutriPROGRAM
636 (AC18/00006), Instituto de Salud Carlos III and co-funded by European Union (ERDF)
637 "A way to make Europe" – ALMA project (PI20/00190) and the European Union’s
638 Horizon 2020 research and innovation program – ATHLETE project (874583). The BiSC
639 cohort was supported by the European Research Council (ERC) under the European
640 Union’s Horizon 2020 research and innovation programme – AirNB project (785994) and
641 the Health Effects Institute (HEI), an organization jointly funded by the United States
642 Environmental Protection Agency (EPA) (R-82811201) and certain motor vehicle and
643 engine manufacturers. We would like to thank all the participants and their families for
644 their generous collaboration. A full list of BiSC researchers can be found at
645 <https://projectebisc.org/en/team/>. Genome-wide genotyping data was funded by the
646 Instituto de Salud Carlos III (ISCIII) and co-funded by European Union (ERDF) "A way
647 to make Europe" – ENTENTE project (PI20/01116) and the Centro Nacional de
648 Genotipado-CEGEN (PRB2-ISCIII). Sofía Aguilar-Lacasaña was funded by the
649 European Union’s Horizon 2020 research and innovation program – ATHLETE project
650 (874583) and the FI-AGAUR Predoctoral contract [2023 FI-2 00797]. Marta Cosin-
651 Tomas was funded by a Beatriu de Pinós Postdoctoral Contract awarded by Generalitat
652 de Catalunya-AGAUR and European Commission-Horizon 2020 (2019 BP 00107).
653 Mireia Gascon holds a Miguel Servet fellowship (Grant CP19/00183) funded by Acción
654 Estratégica de Salud - Instituto de Salud Carlos III, co-funded by European Social Fund

655 “Investing in your future”. We acknowledge support from the grant CEX2023-0001290-
656 S funded by MCIN/AEI/ 10.13039/501100011033, and support from the Generalitat de
657 Catalunya through the CERCA Program.

658 **Ethics approval and consent to participate**

659 From pregnancy up to 18 months’ visits were approved by the Clinical Research Ethics
660 Committee of the Parc de Salut Mar project (2018/8050/I), Medical Research Committee
661 of the Fundació de Gestió Sanitària del Hospital de la Santa Creu i Sant Pau de Barcelona
662 (EC/18/206/5272), and Ethics Committee of the Fundació Sant Joan de Déu (PIC-27-18).
663 Before joining the cohort during their regular first trimester hospital visit, participants
664 were informed by a BiSC midwife or nurse about the study's details, duration, and their
665 option to withdraw without penalty. If they agreed to take part, they signed consent forms
666 permitting the collection of biological samples and genetic studies, receiving a copy for
667 themselves. Parents or legal guardians of children also provided informed consent before
668 any study procedures commenced. Specific consent forms for genetic studies were also
669 provided to mothers and parents or legal guardians of children.

670 **Consent for publication**

671 Not applicable.

672 **Declaration of Competing interests**

673 The authors declare that they have no known competing financial interests or personal
674 relationships that could have appeared to influence the work reported in this paper.

675 **Data availability**

676 Genome-wide DNA methylation summarized results can be found at Zenodo repository
677 (<https://zenodo.org/>) [THIS WILL BE DONE UPON ACCEPTANCE OF THE
678 MANUSCRIPT]. Individual cohort level data may be available by application to the
679 relevant institution after obtaining required approvals. The code for the analyses is

680 available in this GitHub repository link:

681 https://github.com/sofiaguilarl/EWAS_GreenSpace_Placenta.git.

682 **Appendix A. Supplementary tables**

683 **Appendix B. Supplementary figures**

684 **References**

685 Aguilar-Lacasaña, S., Fontes Marques, I., de Castro, M., Dadvand, P., Escribà, X.,
686 Fossati, S., González, J. R., Nieuwenhuijsen, M., Alfano, R., Annesi-Maesano, I.,
687 Brescianini, S., Burrows, K., Calas, L., Elhakeem, A., Heude, B., Hough, A.,
688 Isaevska, E., W V Jaddoe, V., Lawlor, D. A., ... Bustamante, M. (2024). Green space
689 exposure and blood DNA methylation at birth and in childhood – A multi-cohort
690 study. *Environment International*, 188(March), 108684.

691 <https://doi.org/10.1016/j.envint.2024.108684>

692 Alfano, R., Bijmens, E., Langie, S. A. S., Nawrot, T. S., Reimann, B., Vanbrabant, K.,
693 Wang, C., & Plusquin, M. (2023). Epigenome-wide analysis of maternal exposure
694 to green space during gestation and cord blood DNA methylation in the
695 ENVIRONAGE cohort. *Environmental Research*, 216.

696 <https://doi.org/10.1016/j.envres.2022.114828>

697 Baschat, A. A., & Gembruch, U. (2003). The cerebroplacental Doppler ratio revisited.
698 *Ultrasound in Obstetrics & Gynecology*, 21(2), 124–127.

699 <https://doi.org/10.1002/uog.20>

700 Battram, T., Gaunt, T. R., Relton, C. L., Timpson, N. J., & Hemani, G. (2022). A
701 comparison of the genes and genesets identified by GWAS and EWAS of fifteen
702 complex traits. *Nature Communications*, 13(1), 7816.

703 <https://doi.org/10.1038/s41467-022-35037-3>

704 Battram, T., Yousefi, P., Crawford, G., Prince, C., Sheikhali Babaei, M., Sharp, G.,

- 705 Hatcher, C., Vega-Salas, M. J., Khodabakhsh, S., Whitehurst, O., Langdon, R.,
706 Mahoney, L., Elliott, H. R., Mancano, G., Lee, M. A., Watkins, S. H., Lay, A. C.,
707 Hemani, G., Gaunt, T. R., ... Suderman, M. (2022). The EWAS Catalog: a database
708 of epigenome-wide association studies. *Wellcome Open Research*, 7(May), 41.
709 <https://doi.org/10.12688/wellcomeopenres.17598.1>
- 710 Boll, L. M., Khamirchi, R., Alonso, L., Llorba, E., Pozo, Ó. J., Miri, M., & Dadvand, P.
711 (2020). Prenatal greenspace exposure and cord blood cortisol levels: A cross-
712 sectional study in a middle-income country. *Environment International*,
713 144(February), 106047. <https://doi.org/10.1016/j.envint.2020.106047>
- 714 Bowyer, R. C. E., Twohig-Bennett, C., Coombes, E., Wells, P. M., Spector, T. D., Jones,
715 A. P., & Steves, C. J. (2022). Microbiota composition is moderately associated with
716 greenspace composition in a UK cohort of twins. *Science of The Total Environment*,
717 813, 152321. <https://doi.org/10.1016/j.scitotenv.2021.152321>
- 718 Cartographic and Geologic Institute of Catalonia. (2018). Land Cover Map of Catalonia
719 (MCSC) 2018 (Version 1.0) [Dataset]. <https://www.icgc.cat/es/Ambitos-tematicos/Territori-sostenible/Cubiertas-del-suelo>
- 720 [tematicos/Territori-sostenible/Cubiertas-del-suelo](https://www.icgc.cat/es/Ambitos-tematicos/Territori-sostenible/Cubiertas-del-suelo)
- 721 Cartographic and Geologic Institute of Catalonia. (2021). Normalized Difference
722 Vegetation Index (NDVI) 2020 (Version 1.0) [Dataset].
723 <https://ide.cat/geonetwork/srv/eng/catalog.search#/metadata/ndvi-v1r0-2020>
- 724 Castellani, C. A., Longchamps, R. J., Sun, J., Guallar, E., & Arking, D. E. (2020).
725 Thinking outside the nucleus: Mitochondrial DNA copy number in health and
726 disease. *Mitochondrion*, 53(June), 214–223.
727 <https://doi.org/10.1016/j.mito.2020.06.004>
- 728 Cruells, A., Cabrera-Rubio, R., Bustamante, M., Pelegrí, D., Cirach, M., Jimenez-Arenas,
729 P., Samarra, A., Martínez-Costa, C., Collado, M. C., & Gascon, M. (2024). The

730 influence of pre- and postnatal exposure to air pollution and green spaces on infant's
731 gut microbiota: Results from the MAMI birth cohort study. *Environmental*
732 *Research*, 257(June), 119283. <https://doi.org/10.1016/j.envres.2024.119283>

733 Dadvand, P., Gascon, M., Bustamante, M., Rivas, I., Foraster, M., Basagaña, X., Cosín,
734 M., Eixarch, E., Ferrer, M., Gratacós, E., Gómez Herrera, L., Jimenez-Arenas, P.,
735 Júlvez, J., Morillas, À., Nieuwenhuijsen, M. J., Persavento, C., Pujol, J., Querol, X.,
736 Sánchez García, O., ... Zhao, Y. (2024). Cohort Profile: Barcelona Life Study
737 Cohort (BiSC). *International Journal of Epidemiology*, 53(3), 1–9.
738 <https://doi.org/10.1093/ije/dyae063>

739 Delahaye, F., Do, C., Kong, Y., Ashkar, R., Salas, M., Tycko, B., Wapner, R., & Hughes,
740 F. (2018). Genetic variants influence on the placenta regulatory landscape. *PLOS*
741 *Genetics*, 14(11), e1007785. <https://doi.org/10.1371/journal.pgen.1007785>

742 Deyssenroth, M. A., Marsit, C. J., Chen, J., & Lambertini, L. (2020). In-depth
743 characterization of the placental imprintome reveals novel differentially methylated
744 regions across birth weight categories. *Epigenetics*, 15(1–2), 47–60.
745 <https://doi.org/10.1080/15592294.2019.1647945>

746 Dockx, Y., Bijmens, E., Saenen, N., Aerts, R., Aerts, J.-M., Casas, L., Delcloo, A.,
747 Dendoncker, N., Linard, C., Plusquin, M., Stas, M., Van Nieuwenhuysse, A., Van
748 Orshoven, J., Somers, B., & Nawrot, T. (2022). Residential green space in
749 association with the methylation status in a CpG site within the promoter region of
750 the placental serotonin receptor HTR2A. *Epigenetics*, 17(13), 1863–1874.
751 <https://doi.org/10.1080/15592294.2022.2088464>

752 Ernst, J., & Kellis, M. (2017). Chromatin-state discovery and genome annotation with
753 ChromHMM. *Nature Protocols*, 12(12), 2478–2492.
754 <https://doi.org/10.1038/nprot.2017.124>

- 755 Figueras, F., & Gratacós, E. (2014). Update on the diagnosis and classification of fetal
756 growth restriction and proposal of a stage-based management protocol. *Fetal*
757 *Diagnosis and Therapy*, 36(2), 86–98. <https://doi.org/10.1159/000357592>
- 758 Figueras, F., Meler, E., Iraola, A., Eixarch, E., Coll, O., Figueras, J., Francis, A., Gratacos,
759 E., & Gardosi, J. (2008). Customized birthweight standards for a Spanish population.
760 *European Journal of Obstetrics and Gynecology and Reproductive Biology*, 136(1),
761 20–24. <https://doi.org/10.1016/j.ejogrb.2006.12.015>
- 762 Fortin, J.-P., Triche, T. J., & Hansen, K. D. (2017). Preprocessing, normalization and
763 integration of the Illumina HumanMethylationEPIC array with minfi.
764 *Bioinformatics*, 33(4), 558–560. <https://doi.org/10.1093/bioinformatics/btw691>
- 765 Fortin, J. P., Labbe, A., Lemire, M., Zanke, B. W., Hudson, T. J., Fertig, E. J., Greenwood,
766 C. M. T., & Hansen, K. D. (2014). Functional normalization of 450k methylation
767 array data improves replication in large cancer studies. *Genome Biology*, 15(11), 1–
768 17. <https://doi.org/10.1186/s13059-014-0503-2>
- 769 Fowden, A. L., Valenzuela, O. A., Vaughan, O. R., Jellyman, J. K., & Forhead, A. J.
770 (2016). Glucocorticoid programming of intrauterine development. *Domestic Animal*
771 *Endocrinology*, 56, S121–S132. <https://doi.org/10.1016/j.domaniend.2016.02.014>
- 772 Freund, A., Zhong, F. L., Venteicher, A. S., Meng, Z., Veenstra, T. D., Frydman, J., &
773 Artandi, S. E. (2014). Proteostatic control of telomerase function through TRiC-
774 mediated folding of TCAB1. *Cell*, 159(6), 1389–1403.
775 <https://doi.org/10.1016/j.cell.2014.10.059>
- 776 Gascon, M., Cirach, M., Martínez, D., Dadvand, P., Valentín, A., Plasència, A., &
777 Nieuwenhuijsen, M. J. (2016). Normalized difference vegetation index (NDVI) as a
778 marker of surrounding greenness in epidemiological studies: The case of Barcelona
779 city. *Urban Forestry and Urban Greening*, 19, 88–94.

- 780 <https://doi.org/10.1016/j.ufug.2016.07.001>
- 781 Gómez, O., Figueras, F., Fernández, S., Bennasar, M., Martínez, J. M., Puerto, B., &
782 Gratacós, E. (2008). Reference ranges for uterine artery mean pulsatility index at
783 11–41 weeks of gestation. *Ultrasound in Obstetrics & Gynecology*, *32*(2), 128–132.
784 <https://doi.org/10.1002/uog.5315>
- 785 Griffiths, S. K., & Campbell, J. P. (2015). Placental structure, function and drug transfer.
786 *Continuing Education in Anaesthesia Critical Care & Pain*, *15*(2), 84–89.
787 <https://doi.org/10.1093/bjaceaccp/mku013>
- 788 Guo, D. C., Regalado, E. S., Gong, L., Duan, X., Santos-Cortez, R. L. P., Arnaud, P.,
789 Ren, Z., Cai, B., Hostetler, E. M., Moran, R., Liang, D., Estrera, A., Safi, H. J., Leal,
790 S. M., Bamshad, M. J., Shendure, J., Nickerson, D. A., Jondeau, G., Boileau, C., &
791 Milewicz, D. M. (2016). LOX mutations predispose to thoracic aortic aneurysms
792 and dissections. *Circulation Research*, *118*(6), 928–934.
793 <https://doi.org/10.1161/CIRCRESAHA.115.307130>
- 794 Hamada, H., Okae, H., Toh, H., Chiba, H., Hiura, H., Shirane, K., Sato, T., Suyama, M.,
795 Yaegashi, N., Sasaki, H., & Arima, T. (2016). Allele-Specific Methylome and
796 Transcriptome Analysis Reveals Widespread Imprinting in the Human Placenta. *The*
797 *American Journal of Human Genetics*, *99*(5), 1045–1058.
798 <https://doi.org/10.1016/j.ajhg.2016.08.021>
- 799 Hautekiet, P., Saenen, N. D., Aerts, R., Martens, D. S., Roels, H. A., Bijnen, E. M., &
800 Nawrot, T. S. (2022). Higher buccal mtDNA content is associated with residential
801 surrounding green in a panel study of primary school children. *Environmental*
802 *Research*, *213*(February). <https://doi.org/10.1016/j.envres.2022.113551>
- 803 Heikinheimo, V., Tenkanen, H., Bergroth, C., Järv, O., Hiippala, T., & Toivonen, T.
804 (2020). Understanding the use of urban green spaces from user-generated

805 geographic information. *Landscape and Urban Planning*, 201(October 2019).
806 <https://doi.org/10.1016/j.landurbplan.2020.103845>

807 Heiss, J. A., & Just, A. C. (2018). Identifying mislabeled and contaminated DNA
808 methylation microarray data: an extended quality control toolset with examples from
809 GEO. *Clinical Epigenetics*, 10(1), 73. <https://doi.org/10.1186/s13148-018-0504-1>

810 Hemberger, M., Hanna, C. W., & Dean, W. (2020). Mechanisms of early placental
811 development in mouse and humans. *Nature Reviews Genetics*, 21(1), 27–43.
812 <https://doi.org/10.1038/s41576-019-0169-4>

813 Hu, C.-Y., Yang, X.-J., Gui, S.-Y., Ding, K., Huang, K., Fang, Y., Jiang, Z.-X., & Zhang,
814 X.-J. (2021). Residential greenness and birth outcomes: A systematic review and
815 meta-analysis of observational studies. *Environmental Research*, 193(December
816 2020), 110599. <https://doi.org/10.1016/j.envres.2020.110599>

817 Huang, R. C., Melton, P. E., Burton, M. A., Beilin, L. J., Clarke-Harris, R., Cook, E.,
818 Godfrey, K. M., Burdge, G. C., Mori, T. A., Anderson, D., Rauschert, S., Craig, J.
819 M., Kobor, M. S., MacIsaac, J. L., Morin, A. M., Oddy, W. H., Pennell, C. E.,
820 Holbrook, J. D., & Lillycrop, K. A. (2022). Adiposity associated DNA methylation
821 signatures in adolescents are related to leptin and perinatal factors. *Epigenetics*,
822 17(8), 819–836. <https://doi.org/10.1080/15592294.2021.1876297>

823 Huypens, P., Pillai, R., Sheinin, T., Schaefer, S., Huang, M., Odegaard, M. L.,
824 Ronnebaum, S. M., Wettig, S. D., & Joseph, J. W. (2011). The dicarboxylate carrier
825 plays a role in mitochondrial malate transport and in the regulation of glucose-
826 stimulated insulin secretion from rat pancreatic beta cells. *Diabetologia*, 54(1), 135–
827 145. <https://doi.org/10.1007/s00125-010-1923-5>

828 *isglobal-brge/EASIER: Tools for methylation data analysis*. (2022).
829 <https://github.com/isglobal-brge/EASIER>

- 830 Johnson, W. E., Li, C., & Rabinovic, A. (2007). Adjusting batch effects in microarray
831 expression data using empirical Bayes methods. *Biostatistics*, 8(1), 118–127.
832 <https://doi.org/10.1093/biostatistics/kxj037>
- 833 Juliusdottir, T., Steinhorsdottir, V., Stefansdottir, L., Sveinbjornsson, G., Ivarsdottir, E.
834 V., Thorolfsdottir, R. B., Sigurdsson, J. K., Tragante, V., Hjorleifsson, K. E.,
835 Helgadottir, A., Frigge, M. L., Thorgeirsson, G., Benediktsson, R., Sigurdsson, E.
836 L., Arnar, D. O., Steingrimsdottir, T., Jonsdottir, I., Holm, H., Gudbjartsson, D. F.,
837 Stefansson, K. (2021). Distinction between the effects of parental and fetal genomes
838 on fetal growth. *Nature Genetics*, 53(8), 1135–1142.
839 <https://doi.org/10.1038/s41588-021-00896-x>
- 840 Kanehisa, M. (2000). KEGG: Kyoto Encyclopedia of Genes and Genomes. *Nucleic Acids*
841 *Research*, 28(1), 27–30. <https://doi.org/10.1093/nar/28.1.27>
- 842 Lawrence, M., Huber, W., Pagès, H., Aboyoun, P., Carlson, M., Gentleman, R., Morgan,
843 M. T., & Carey, V. J. (2013). Software for Computing and Annotating Genomic
844 Ranges. *PLoS Computational Biology*, 9(8), 1–10.
845 <https://doi.org/10.1371/journal.pcbi.1003118>
- 846 Lent, S., Cardenas, A., Rifas-Shiman, S. L., Perron, P., Bouchard, L., Liu, C. T., Hivert,
847 M. F., & Dupuis, J. (2021). Detecting differentially methylated regions with multiple
848 distinct associations. *Epigenomics*, 13(6), 451–464. [https://doi.org/10.2217/epi-](https://doi.org/10.2217/epi-2020-0344)
849 [2020-0344](https://doi.org/10.2217/epi-2020-0344)
- 850 Maccani, M. A., & Marsit, C. J. (2009). Epigenetics in the Placenta. *American Journal of*
851 *Reproductive Immunology*, 62(2), 78–89. [https://doi.org/10.1111/j.1600-](https://doi.org/10.1111/j.1600-0897.2009.00716.x)
852 [0897.2009.00716.x](https://doi.org/10.1111/j.1600-0897.2009.00716.x)
- 853 Markevych, I., Schoierer, J., Hartig, T., Chudnovsky, A., Hystad, P., Dzhambov, A. M.,
854 de Vries, S., Triguero-Mas, M., Brauer, M., Nieuwenhuijsen, M. J., Lupp, G.,

- 855 Richardson, E. A., Astell-Burt, T., Dimitrova, D., Feng, X., Sadeh, M., Standl, M.,
856 Heinrich, J., & Fuertes, E. (2017). Exploring pathways linking greenspace to health:
857 Theoretical and methodological guidance. *Environmental Research*, *158*(February),
858 301–317. <https://doi.org/10.1016/j.envres.2017.06.028>
- 859 Mizuarai, S., Miki, S., Araki, H., Takahashi, K., & Kotani, H. (2005). Identification of
860 dicarboxylate carrier Slc25a10 as malate transporter in de Novo fatty acid synthesis.
861 *Journal of Biological Chemistry*, *280*(37), 32434–32441.
862 <https://doi.org/10.1074/jbc.M503152200>
- 863 Mortillo, M., & Marsit, C. J. (2022). Select Early-Life Environmental Exposures and
864 DNA Methylation in the Placenta. *Current Environmental Health Reports*, *10*(1),
865 22–34. <https://doi.org/10.1007/s40572-022-00385-1>
- 866 Nwanaji-Enwerem, U., McGeary, J. E., & Grigsby-Toussaint, D. S. (2024). Greenspace,
867 stress, and health: how is epigenetics involved? *Frontiers in Public Health*,
868 *12*(February), 1–5. <https://doi.org/10.3389/fpubh.2024.1333737>
- 869 Ohgane, J., Yagi, S., & Shiota, K. (2008). Epigenetics: The DNA Methylation Profile of
870 Tissue-Dependent and Differentially Methylated Regions in Cells. *Placenta*,
871 *29*(SUPPL.), 29–35. <https://doi.org/10.1016/j.placenta.2007.09.011>
- 872 Paterson, H. A. B., Yu, S., Artigas, N., Prado, M. A., Haberman, N., Wang, Y. F., Jobbins,
873 A. M., Pahita, E., Mokochinski, J., Hall, Z., Guerin, M., Paulo, J. A., Ng, S. S.,
874 Villarroya, F., Rashid, S. T., Le Goff, W., Lenhard, B., Cebola, I., Finley, D., ...
875 Vernia, S. (2022). Liver RBFOX2 regulates cholesterol homeostasis via Scarb1
876 alternative splicing in mice. *Nature Metabolism*, *4*(12), 1812–1829.
877 <https://doi.org/10.1038/s42255-022-00681-y>
- 878 Schroeder, D. I., Blair, J. D., Lott, P., Yu, H. O. K., Hong, D., Crary, F., Ashwood, P.,
879 Walker, C., Korf, I., Robinson, W. P., & LaSalle, J. M. (2013). The human placenta

- 880 methylome. *Proceedings of the National Academy of Sciences*, *110*(15), 6037–6042.
- 881 <https://doi.org/10.1073/pnas.1215145110>
- 882 Shi, H., Yuan, X., Yang, X., Huang, R., Fan, W., & Liu, G. (2024). A novel diabetic foot
883 ulcer diagnostic model: identification and analysis of genes related to glutamine
884 metabolism and immune infiltration. *BMC Genomics*, *25*(1), 125.
885 <https://doi.org/10.1186/s12864-024-10038-2>
- 886 Spanish National Institute of Statistics. Atlas of Household Income Distribution 2023;
887 https://www.ine.es/metodologia/metodologia_adrh.pdf. Accessed July 1, 2024
- 888 Suderman, M., Staley, J. R., French, R., Arathimos, R., Simpkin, A., & Tilling, K. (2018).
889 Dmrff: Identifying Differentially Methylated Regions Efficiently With Power and
890 Control. *BioRxiv (Preprint)*, *1*, 1–26. <https://doi.org/10.1101/508556>
- 891 Teschendorff, A. E., Marabita, F., Lechner, M., Bartlett, T., Tegner, J., Gomez-Cabrero,
892 D., & Beck, S. (2013). A beta-mixture quantile normalization method for correcting
893 probe design bias in Illumina Infinium 450 k DNA methylation data. *Bioinformatics*,
894 *29*(2), 189–196. <https://doi.org/10.1093/bioinformatics/bts680>
- 895 Triche, T. J., Weisenberger, D. J., Van Den Berg, D., Laird, P. W., & Siegmund, K. D.
896 (2013). Low-level processing of Illumina Infinium DNA Methylation BeadArrays.
897 *Nucleic Acids Research*, *41*(7), e90–e90. <https://doi.org/10.1093/nar/gkt090>
- 898 Tucker, C. J. (1979). Red and photographic infrared linear combinations for monitoring
899 vegetation. *Remote Sensing of Environment*, *8*(2), 127–150.
900 [https://doi.org/10.1016/0034-4257\(79\)90013-0](https://doi.org/10.1016/0034-4257(79)90013-0)
- 901 Welburn, J. P. I., Grishchuk, E. L., Backer, C. B., Wilson-Kubalek, E. M., Yates, J. R.,
902 & Cheeseman, I. M. (2009). The Human Kinetochore Skl Complex Facilitates
903 Microtubule Depolymerization-Coupled Motility. *Developmental Cell*, *16*(3), 374–
904 385. <https://doi.org/10.1016/j.devcel.2009.01.011>

- 905 Wu, X., Xie, C., Zhang, Y., Fan, Z., Yin, Y., & Blachier, F. (2015). Glutamate-glutamine
906 cycle and exchange in the placenta-fetus unit during late pregnancy. *Amino Acids*,
907 *47*(1), 45–53. <https://doi.org/10.1007/s00726-014-1861-5>
- 908 Xiong, M., Li, L., Wen, L., & Zhao, A. (2024). Decidual stromal cell–derived exosomes
909 deliver miR-22-5p_R-1 to suppress trophoblast metabolic switching from
910 mitochondrial respiration to glycolysis by targeting PDK4 in unexplained recurrent
911 spontaneous abortion. *Placenta*, *153*(December 2023), 1–21.
912 <https://doi.org/10.1016/j.placenta.2024.05.131>
- 913 Yu, J., Duan, Y., Lu, Q., Chen, M., Ning, F., Ye, Y., Lu, S., Ou, D., Sha, X., Gan, X.,
914 Zhao, M., & Lash, G. E. (2024). Cytochrome c oxidase IV isoform 1 (COX4-1)
915 regulates the proliferation, migration and invasion of trophoblast cells via
916 modulating mitochondrial function. *Placenta*, *151*(February), 48–58.
917 <https://doi.org/10.1016/j.placenta.2024.04.011>
- 918 Yuan, V., Hui, D., Yin, Y., Peñaherrera, M. S., Beristain, A. G., & Robinson, W. P.
919 (2021). Cell-specific characterization of the placental methylome. *BMC Genomics*,
920 *22*(1), 6. <https://doi.org/10.1186/s12864-020-07186-6>
- 921 Yuan, Y., Huang, F., Lin, F., Zhu, P., & Zhu, P. (2020). Green space exposure on
922 mortality and cardiovascular outcomes in older adults: a systematic review and
923 meta-analysis of observational studies. *Aging Clinical and Experimental Research*,
924 *0123456789*. <https://doi.org/10.1007/s40520-020-01710-0>
- 925 Zare Sakhvidi, M. J., Mehrparvar, A. H., Zare Sakhvidi, F., & Dadvand, P. (2023).
926 Greenspace and health, wellbeing, physical activity, and development in children
927 and adolescents: An overview of the systematic reviews. *Current Opinion in*
928 *Environmental Science & Health*, *32*, 100445.
929 <https://doi.org/10.1016/j.coesh.2023.100445>

930 Zhou, W., Triche, T. J., Laird, P. W., & Shen, H. (2018). SeSAME: reducing artifactual
931 detection of DNA methylation by Infinium BeadChips in genomic deletions. *Nucleic
932 Acids Research*, 46(20), 1–15. <https://doi.org/10.1093/nar/gky691>
933